Quantum Electronics **41** (4) 377–381 (2011)

PACS numbers: 52.38.Ph; 52.50.Jm; 42.65.Re
DOI: 10.1070/QE2011v041n04ABEH014501

Simulations of neutron emission in the irradiation of deuterated polyethylene by ultrahigh-intensity laser pulses

S.N. Andreev, S.G. Garanin, A.A. Rukhadze, V.P. Tarakanov, B.P. Yakutov

Abstract. **The neutron yield from deuterated polyethylene targets irradiated by ultrahigh-intensity laser pulses was calculated in a wide range of pulse energies. The resultant data are in better agreement with available experimental data than the data of the corresponding simulations performed by other authors earlier. The neutron pulse duration was shown to exceed the laser pulse duration by more than an order of magnitude. We also showed that the neutron yield accompanying the irradiation of a laminated target of deuterated polyethylene is, thanks to redistribution of deuteron fluxes in its volume, substantially higher in comparison with the irradiation of a continuous target.**

Keywords: *laser-produced plasma, neutrons, laminated target.*

1. Introduction

In the past decade, considerable attention was given to experimental and theoretical investigations of nuclear reactions occurring when ultrahigh-intensity ($10^{18}-10^{20}$ W cm^{-2}) subpicosecond (0.1–1 ps) laser pulses irradiate solid [1], cluster [2], and gaseous [3] targets which contain deuterium.

High-energy (fast) deuterons produced under laser irradiation undergo a fusion reaction D(d, n)^{3}He (D–D reaction) attended with a neutron yield. Measuring the parameters of such neutrons is an efficient method of studying the fast deuterons, especially those which were accelerated into the target interior under the action of a laser pulse. To acquire quantitative information about the energy spectrum and angular distribution of fast deuterons proceeding from the research data on neutron fluxes, Hilscher et al. [4] and Izumi et al. [5] developed an approach whereby the deuteron motion in the target volume was modelled by the Monte Carlo technique with the inclusion of ionisation losses and neutron emission. The ionisation losses were taken into account by introducing an empirical “decelerating force” acting on a deuteron in its propagation through the target volume.

S.N. Andreev, A.A. Rukhadze A.M. Prokhorov General Physics Institute, Russian Academy of Sciences, ul. Vavilova 38, 119991 Moscow, Russia; e-mail: andreevsn@ran.gpi.ru, rukh@fpl.gpi.ru;
S.G. Garanin, B.P. Yakutov Research Institute of Laser Physics, Russian Federal Nuclear Centre ‘All-Russian Scientific Research Institute of Experimental Physics’, ul. Mira 37, 607190 Sarov, Nizhnii Novgorod region, Russia; e-mail: garanin@otd13.vniief.ru, Boris_Yakutov@mail.ru;
V.P. Tarakanov Joint Institute for High Temperatures, Russian Academy of Sciences, ul. Izhorskaya 13/19, 125412 Moscow, Russia; e-mail: karat@tarak.msk.ru

Received 17 November 2010; revision received 17 February 2011
Kvantovaya Elektronika **41** (4) 377–381 (2011)
Translated by E.N. Ragozin

A similar approach was adopted by Toupin et al. [6] and by Petrov and Davis [7], who performed a numerical investigation into the effect of different parameters of the laser pulse and the target on the emission of neutrons. The virtually similar simulation models employed in these works incorporated a two-dimensional PIC code (it was used to calculate the velocity distribution function for the fast deuterons accelerated during laser irradiation) and a postprocessor, which used the resultant distribution function as the initial condition for calculating the neutron emission in the interaction of the fast deuterons with the stationary deuterons of the target. In this case, the mathematical model of the postprocessor [6, 7] relied on the following basic assumptions: the angular deuteron distribution is symmetrical relative to the axis of the laser pulse; the target is sufficiently ‘thick,’ so that all fast deuterons lose their energy completely for the ionisation of atoms in the target volume.

One of the disadvantages of the model of Refs [6, 7], which is indicated by the authors of Ref. [6] themselves, is that there is no way of taking into account the dynamics of the heating of target atoms in their interaction with electron and deuteron beams accelerated by the laser pulse. We also emphasise that the postprocessor does not in principle permit modelling the emission of neutrons in the interaction of counter-propagating beams, which may emerge under laser irradiation of structurally complex targets, in particular hollow and laminated targets.

In this work we propose an approach involving *ab initio* calculations of the D–D reaction event probability at each time step for every deuteron in the course of self-consistent PIC simulations of the ultrahigh-intensity laser pulse interaction with a target containing deuterium ions. This approach was realised in the framework of a fully three-dimensional relativistic electromagnetic PIC code termed KARAT [8, 9].

As shown in our work, not only does the proposed neutron emission simulation method enable obtaining data which agree well with experimental data on neutron emission in the irradiation of ‘thick’ deuterated polyethylene targets, but it also enables investigating laminated targets, in which the neutron yield is substantially higher.

2. Unit which describes neutron emission in the course of D–D reaction

The mathematical model of neutron emission unit incorporated into the KARAT code relies on the formula for the cross section of the fusion reaction D + D $\rightarrow$ ^{3}He + n in the laboratory reference frame. In accordance with the well-known semiempirical data of Ref. [10] this formula is written in the following form:

$$\sigma_{\rm dd}(E_0) = \frac{107.4 + 0.33E_0}{E_0}\exp\left(-\frac{44.4}{\sqrt{E_0}}\right), \quad (1)$$

where E_0 is the fast deuteron energy expressed in kiloelectronvolts; $\sigma_{\rm dd}$ is the cross section in barns (1 barn is equal to 10^{-24} cm^2).

In the course of simulation of the action of an ultrahigh-intensity laser pulse on a deuteron-bearing target, at each time step the probability of a fusion reaction event for every primary deuteron-corresponding macroparticle travelling with velocity $\boldsymbol{V}$ is defined as follows. Calculated at every mesh node of the simulation region are the deuteron density $n_{\rm d}$, the average deuteron velocity $\boldsymbol{V}_{\rm av}$, and the rms velocity spread $\boldsymbol{V}_T$ in every Cartesian coordinate in the reference frame travelling with velocity $\boldsymbol{V}_{\rm av}$. Determined next is the relative velocity $\boldsymbol{V}_{\rm rel}$ of the primary deuteron and a random target deuteron at this node.

$$\boldsymbol{V}_{\rm rel} = \boldsymbol{V} - \boldsymbol{V}_{\rm av} - \boldsymbol{V}_T(\chi - 0.5), \quad (2)$$

where χ is a random number from the interval 0–1. Formula (1) is used to calculate the total reaction cross section σ for the kinetic energy E_0 corresponding to this velocity and, finally, the probability P is found:

$$P = A\sigma|V_{\rm rel}|n_{\rm d}\Delta t, \quad (3)$$

where Δt is a time step. The presence of the second term in formula (2) ensures the absence of D–D reactions, for instance, in a monoenergetic deuteron beam, when $\boldsymbol{V} = \boldsymbol{V}_{\rm av}$. The presence of the third term in this formula permits us to take into account in formula (3) the heating of target deuterons due to laser irradiation. No limitations are imposed on the values of velocities $\boldsymbol{V}_{\rm av}$ and $\boldsymbol{V}_T$ in formula (2). Since the reaction probability is expected to be quite low for the expected values of the physical parameters of the objects being simulated, to create favourable conditions for the observation of neutron dynamics we introduced into formula (3) a coefficient A for the artificial augmentation of reaction probability. In the determination of the real neutron yield, the number of neutrons obtained from simulations is divided by this coefficient.

The probability calculated by formula (3) is compared with the random number from the 0–1 interval; when this probability is smaller than this number, a passage to the next deuteron is effected. Otherwise there unfolds the event of 2.45-MeV neutron production. Initially, a deuteron closest to the primary one is found whose relative kinetic energy is close to the energy employed in the calculation of the probability. Next, a neutron is projected from the centre-of-mass point of the primary and closest deuterons. In the centre-of-mass reference frame, the neutron is projected with a velocity corresponding to an energy of 2.45 MeV and at an angle uniformly distributed from 0 to 2π rad [11]. On launching the neutron, its trajectory is calculated up to the point of intersection with the boundary of the simulation region, where its parameters are registered. The neutron is assumed to experience no interactions inside the simulation region.

Also projected from the point of neutron launch is a macroparticle, which models a $^3{\rm He}^{2+}$ ion. Its momentum is computed from the requirement of momentum conservation in the event being described.

3. Simulations of neutron emission in the laser irradiation of deuterated polyethylene targets

To test the neutron emission unit we performed simulations of deuterated polyethylene target irradiation by a femtosecond laser pulse corresponding to the simulation reported in Ref. [7]. The parameters of the simulation region, the target, and the laser pulse approximated, insofar as possible, the parameters employed in Ref. [7]. Our simulation was carried out with the aid of the two-dimensional XZ version of the PIC KARAT code, whose physical model is outlined, for instance, in Ref. [9].

The simulation region was an xz square with sides of length 20 μm. The step of grid was equal to 20 nm in both directions. The laser pulse was incident on the left boundary of the simulation region and propagated in the positive direction of the z axis. The boundary conditions for electric and magnetic fields at the left and right boundaries of the simulation region ensured the input and output of the radiation. The boundary conditions at the upper and lower boundaries of the simulation region corresponded to the conditions at a perfectly conducting surface. All boundaries of the simulation region were absorptive for macroparticles.

The target was a layer of deuterated polyethylene $(CD_2)_n$ of thickness l_0 = 4 μm and width d_0 = 12 μm, which occupied the region from z = 5 μm to z = 9 μm and from x = 4 μm to x = 16 μm. Since the energy of particle motion in the field of the laser pulse involved exceeded the electron binding energy in the solid target by many orders of magnitude, the target was modelled as a uniform collisionless plasma with the density of a solid corresponding to the deuterated polyethylene density $\rho_{\rm PE}$ = 1.105 g cm^{-3}. The plasma consisted of electrons with a density $n_{\rm e} = 1.64\times10^{23}$ cm^{-3}, C^{2+} carbon ions with a mass $12m_{\rm p}$ and a density $n_{\rm C} = 4.11\times10^{22}$ cm^{-3}, and deuterons D^+ with a mass $2m_{\rm p}$ and a density $n_{\rm d} = 8.22\times10^{22}$ cm^{-3}, where $m_{\rm p}$ is the proton mass.

The target was irradiated along the normal to its surface by linearly polarised laser radiation with a wavelength λ = 1 μm, a dimension of the Gaussian irradiation spot r_0 = 3 μm centred at a point x = 10 μm, and a pulse duration τ_0 = 160 fs. The laser pulse intensity varied in time in accordance with the formula $I(t) = I_0\sin^2(\pi t/\tau_0)$, where $I_0 = 10^{20}$ W cm^{-2}.

Since the simulation was carried out in the two-dimensional geometry, the third dimension (along the y axis) formally remained unused. This is the reason why such parameters as the total energy of laser radiation, the kinetic energy of particles, the neutron yield, etc. were determined per unit length (1 cm) along the y axis. Assuming, following the authors of Ref. [7], that the spot of laser radiation pulse is round, we introduce a dimensional factor $\sqrt{\pi}r_0 = 5.3\times10^{-4}$ cm to convert the dimensions of these quantities to their natural dimension. In particular, in this case the total energy of incident laser radiation $E_{\rm las} = \pi r_0^2 I_0\tau_0/2$ = 2.26 J and the total number of deuterons $N_{\rm d} = n_{\rm d}l_0d_0\sqrt{\pi}r_0 = 2.1\times10^{13}$.

Figure 1 shows the time dependences of the total kinetic energy of electrons (e^-), deuterons (D^+), and carbon ions (C^{2+}) obtained by simulations. For comparison, the dashed line shows the temporal profile of the intensity of the laser pulse (in relative units along the ordinate axis). The point in time t = 0 corresponds to the arrival of the laser pulse at the target surface.

Referring to Fig. 1, the total kinetic energy of electrons attains its peak value on the trailing edge of the laser pulse; after this it begins to subside. The ion energy rises with time

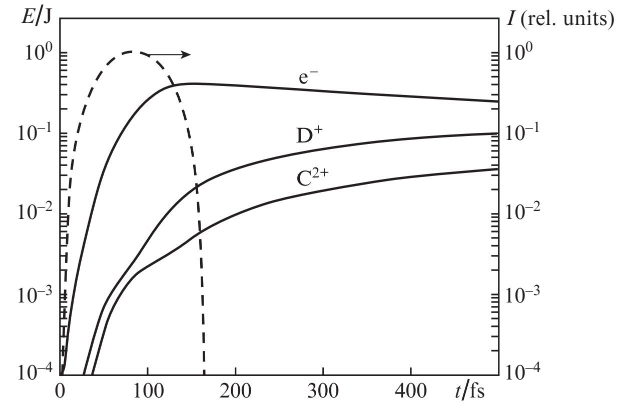

Figure 1. Total electron (e^-), deuteron (D^+) and carbon ion (C^{2+}) kinetic energies as functions of time. The dashed curve shows the temporal intensity profile of the laser pulse.

and saturates approximately 0.5 ps after the cessation of the laser pulse. At the point in time $t = 240$ fs, at which the simulation of Ref. [7] terminates, the total kinetic energy of deuterons was equal to 47 mJ (which is approximately 2.3 time higher than in Ref. [7]). By the point in time $t = 800$ fs it amounted to 115 mJ. In this case, the efficiency of laser radiation conversion to the kinetic energy of deuterons was equal to 5%. The highest energy of individual deuterons exceeded 11 MeV (8 MeV in Ref. [7]). Therefore, according to our simulations the deuterons gain approximately 5 times higher energy than in Ref. [7], but during a longer period. It is pertinent to note that a relatively longer duration of ion acceleration upon cessation of the laser pulse was pointed out earlier, for instance by Oishi et al. [12] and by Andreev and Tarakanov [13].

Let us consider in greater detail the features of deuteron acceleration under target irradiation. Figure 2 shows the distribution of the z-components of deuteron velocities at the point in time $t = 250$ fs. Three deuteron fluxes result from the laser irradiation of the target: deuterons which move from the front target surface in the opposite direction to the laser pulse (1), deuterons which move towards the target interior (2), and

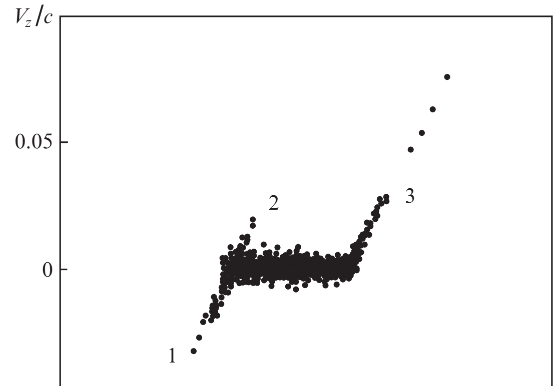

Figure 2. Distribution of z velocity components for deuterons at the point in time $t = 250$ fs.

deuterons which travel from the rear target surface in the direction of laser pulse propagation (3).

One can see from Fig. 2 that only a small fraction of deuterons experiences acceleration: at the front and rear surfaces of the target, while the majority of deuterons in its volume remain cool (by the point in time $t = 250$ fs the average kinetic energy of the in-target deuterons amounts to only 13 keV). Furthermore, only the deuterons of group 2, which travel in the target volume, may effectively participate in the D–D reaction with cool target deuterons, while the deuterons of groups 1 and 3, despite their high energy, cannot make an appreciable contribution to the neutron yield.

In a paper by Wilks et al. [14] and in a number of subsequent papers (see, for instance, Ref. [13] and references therein) it was shown that the main mechanism responsible for the acceleration of ions into the target interior is the light pressure of the laser pulse in its reflection from the target surface. An analysis of the deuteron energy distribution function obtained in our simulations suggests that the fraction of fast deuterons in the target volume with energies exceeding 300 keV amounted to 0.5% of the total number of deuterons. Therefore, the number of fast deuterons in the target volume, which participated effectively in the D–D reaction, was equal to $\sim 10^{11}$. It is noteworthy that a similar estimate of the amount of fast deuterons under the similar parameters of the laser pulse and the target was given by Disdier et al. [15] and Belyaev et al. [16]. In Ref. [7], the number of deuterons with energies above 1 MeV was estimated at about 10^{11}.

In the motion of deuterons through the target volume there occurred D–D reaction events, resulting in the production of neutrons in accordance with the model described in Section 2 of the present work. Figure 3 shows the time dependences of the total neutron fluxes F on the left and right boundaries as well as on the upper and lower boundaries of the simulation region.

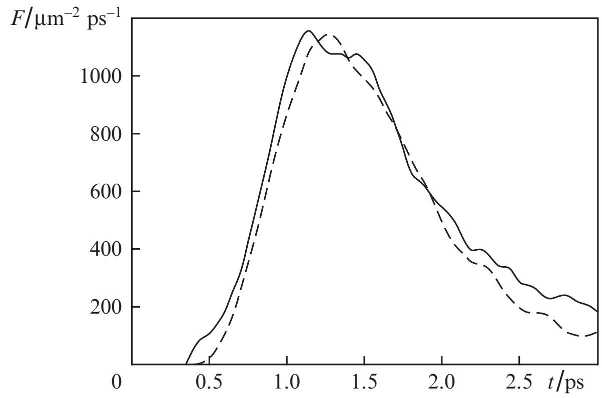

Figure 3. Time dependences of the total neutron fluxes: the solid curve depicts the fluxes on the left and right boundaries of the computational domain, the dashed curve stands for the fluxes on the upper and lower boundaries.

As is evident from Fig. 3, neutrons begin to arrive at the boundaries of the simulation region approximately 300 fs after the termination of laser target irradiation. The neutron fluxes build up for 1.5 ps to reach its peak and then fall off practically to zero during the following 1.5 ps. As this takes place, the total neutron flux on the left and right boundaries turns out to be somewhat higher (by a factor of 1.1) than the flux on the upper and lower boundaries of the simulation region. This is consistent with the findings of Refs [4–7], which pointed out the anisotropy of neutron emission in the ultrahigh-intensity laser irradiation of deuterated targets.

Investigations of the dependence of the neutron yield on the intensity and duration of the laser pulse for an invariable area of the irradiation spot, which were performed in Ref. [7], showed that the neutron yield was determined by the energy E_{las} of the incident laser pulse. This dependence is plotted in Fig. 4.

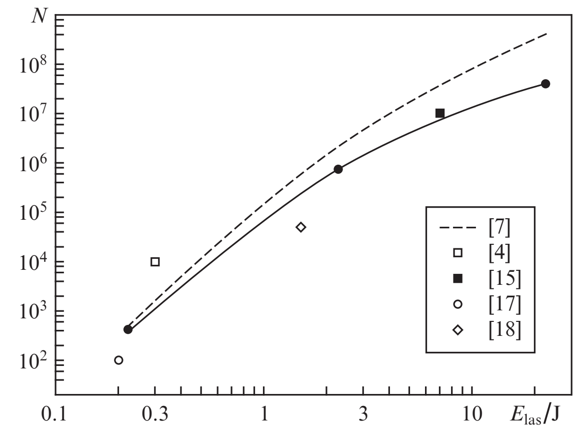

Figure 4. Neutron yield N as a function of the energy E_{las} of the incident laser pulse. The solid curve with black points represents the data of simulations performed with the KARAT code for intensities of the incident laser pulse of 10^{19}, 10^{20}, and 10^{21} W cm^{-2} (the remaining parameters of the simulations remained invariable in this case); the dashed curve represents the simulations of Ref. [7]; the points show the results of experiments in laser irradiation of targets of deuterated polyethylene $(CD_2)_n$ carried out in Refs [4, 15, 17, 18].

One can see that the results of our simulations are in good agreement with those of Ref. [7] and the well-known experimental data in a wide range (0.2–10 J) of energies of the incident laser pulse. The difference in neutron yield between our simulation and that of Ref. [7], which accumulates with increasing laser energy for $E_{las} > 10$ J, can supposedly be attributed to the difference in approaches to the modelling of D–D reactions. Our 'discreet' approach implies that the high-energy deuteron vanishes in a D–D reaction event; by contrast, in Ref. [7] the deuteron continues to make contributions to the neutron yield while travelling through the target volume until it stops completely due to ionisation losses. For low deuteron energies (below 300 keV), when the D–D reaction cross section tends to zero, both approaches yield similar results. However, as the deuteron energy and the D–D reaction cross section increase, the approach adopted in Ref. [7] begins to yield higher neutron yields than our simulation.

It is pertinent to note that the experimental conditions of Refs [4, 15, 17, 18] vary widely in intensity and duration of the laser pulse as well as in amount of the preplasma at the target surface. Since the preplasma has a significant effect on the dynamics of ion acceleration at the front target surface [13], the neutron yield should depend on its parameters. Indeed, in Ref. [7] it is pointed out that the presence of the preplasma with a characteristic length of 0.1–0.3 μm results in an increase in neutron yield in comparison with the target void of the preplasma, but further increase in characteristic length of the preplasma appreciably lowers the neutron yield. Conceivably this is the reason why the neutron yield in Ref. [17] was lower than the data of our simulations and of Ref. [7].

4. The case of laminated target of deuterated polyethylene

Petrov and Davis [7] pointed out that the neutron emission efficiency is appreciably higher when an ultrahigh-intensity laser pulse irradiates a thin two-layer target: a gold foil with a layer of deuterium deposited on its rear side. The directional deuteron flux produced by laser irradiation bombarded the surface of the second, 'thick,' target of deuterated polyethylene and gave rise to neutron emission in the course of D–D reaction. Similar directional deuteron fluxes are also produced in the case considered above (see fluxes 1 and 3 in Fig. 2); however, they do not result in neutron emission, because they do not interact with the stationary deuterons of the target or with counterpropagating deuteron fluxes. The use of laminated targets makes it possible to ensure the interaction deuteron fluxes.

Figure 5a shows the schematic of the simulation region in the irradiation of a laminated target of deuterated polyethylene by an ultrahigh-intensity laser pulse. The laser pulse and the target parameters correspond exactly to the case considered in Section 3, except that the target is divided into eight equal 0.5-μm-thick layers spaced at 0.5 μm in the positive direction of the z axis. The intensity of the laser pulse $I_0 = 10^{20}$ W cm-2.

Figure 5b shows the distribution of the z-components of deuteron velocities in the laminated target at the point in time $t = 250$ fs. One can see that deuteron fluxes similar to fluxes 1 and 3 in Fig. 2 are now formed in every target layer. The deuteron flux from the front surface of the first (left) layer in the opposite direction to the incident laser pulse, which is similar to flux 1 in Fig. 2, does not make a contribution to neutron emission as before. In this case, the deuteron flux from the rear surface of the last layer, which does not make a contribution to the neutron yield, is substantially lower than its corresponding flux 3 in Fig. 2. Therefore, the target layering made it possible to redistribute the deuteron fluxes in such a way that the number of accelerated deuterons moving inside the laminated target became substantially larger.

From the simulations performed in our work it follows that the neutron yield in the irradiation of the laminated target is 2.8 times higher than in the case of a continuous target considered above and is equal to 2.1×10^6 neutrons. The anisotropy of angular neutron distribution also became more pronounced: the ratio of the total neutron flux on the left and right boundaries to the flux on the upper and lower boundaries of the simulation region became equal to 1.22.

It is noteworthy that the laminated target parameters like the number of layers, their thickness, and their spacing have a significant effect on the dynamics of deuterons and the neutron emission. Indeed, with decreasing the number of layers and their spacing the laminated target will structurally approach a continuous target and the neutron yield will become lower. On the other hand, increasing the number of layers and their spacing will result in a lowering of the effective deuteron density in the target and the consequential lowering of the D–D reaction probability [see formula (3)]. Therefore, there exists a set of target parameters whereby the neutron yield attains its peak value. Investigation of neutron emission in relation to the target parameters is of unquestionable interest for optimising the yield and angular distribution of neutrons.

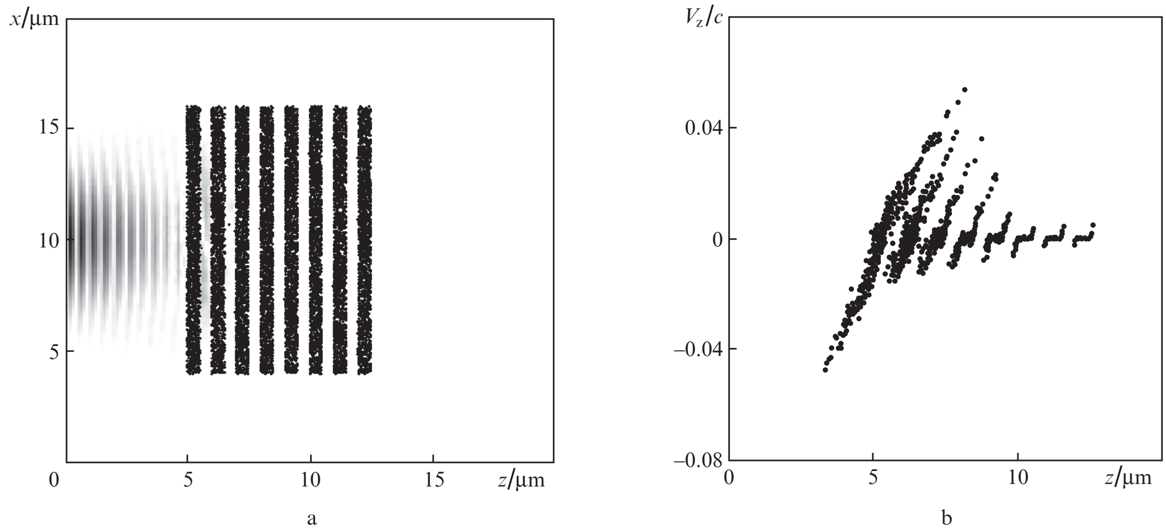

Figure 5. Schematic representation of the computational domain (a) and distribution of the z-components of deuteron velocities at the point in time t = 250 fs (b) in the irradiation of a laminated target of deuterated polyethylene by an ultrahigh-intensity laser pulse.

5. Conclusions

In the present work we performed simulations of neutron emission in the irradiation of deuterated polyethylene targets by ultrahigh-intensity laser pulses with the use of a novel technique, whereby the probability of D–D reaction events is determined by *ab initio* calculations for every deuteron at each time step. The employment of this technique allowed us to calculate the spatio-temporal characteristics of the neutron pulse formed in the laser irradiation of the deuterated polyethylene target; the duration of the neutron pulse exceeded the duration of the laser pulse by more than an order of magnitude and was equal to ~3 ps. The total neutron yield is in good agreement with the experimental data of Refs [4, 15, 17, 18] in the 0.2–10 J energy range of incident laser pulses.

We considered the emission of neutrons in the interaction of counter-propagating deuteron beams produced in the interaction of a laminated deuterated polyethylene target by an ultrahigh-intensity laser pulse. The neutron yield in the irradiation of the laminated target was shown to be substantially (2.8 times) higher than in the irradiation of the continuous deuterated polyethylene target due to redistribution of deuteron fluxes, all other conditions being equal.

Acknowledgements. This work was supported by the Foundation of the President of the Russian Federation for the Support of Young Russian Scientists (Grant No. MK-6184.2010.2).

References

1. Norreys P.A. et al. *Plasma Phys. Controlled Fusion*, **40**, 175 (1998).
2. Madison K.W. et al. *Phys. Plasmas*, **11**, 270 (2004).
3. Fritzler S. et al. *Phys. Rev. Lett.*, **89**, 165004 (2002).
4. Hilscher D. et al. *Phys. Rev. E*, **64**, 016414 (2001).
5. Izumi N. et al. *Phys. Rev. E*, **65**, 036413 (2002).
6. Toupin C., Lefebvre E., Bonnaud G. *Phys. Plasmas*, **8**, 1011 (2001).
7. Petrov G.M., Davis J. *Phys. Plasmas*, **15**, 073109 (2008).
8. Tarakanov V.P. *User's Manual for Code KARAT* (USA, VA: Berkeley Research Associates Inc., 1992).
9. Andreev S.N., Rukhadze A.A., Tarakanov V.P., Yakutov B.P. *Kvantovaya Elektron.*, **40**, 64 (2010) [*Quantum Electron.*, **40**, 64 (2010)].
10. Bosch H.S., Hale G.M. *Nucl. Fusion*, **31**, 611 (1992).
11. Akhiezer A.I., Pomeranchuk I.Ya. *Nekotorye Voprosy Teorii Yadra* (Some Problems of Nuclear Theory) (Moscow-Leningrad: Gostekhizdat, 1950).
12. Oishi Y. et al. *Phys. Plasmas*, **12**, 073102 (2005).
13. Andreev S.N., Tarakanov V.P. *Fiz. Plazmy*, **35**, 1094 (2009).
14. Wilks S.C., Kruer W.L., Tabak M., Langdon A.B. *Phys. Rev. Lett.*, **69**, 1383 (1992).
15. Disdier L., Garconnet J-P., Malka G., Miquel J-L. *Phys. Rev. Lett.*, **82**, 1454 (1999).
16. Belyaev V.S. et al. *Yadernaya Fizika*, **72**, 1123 (2009).
17. Pretzler G. et al. *Phys. Rev. E*, **58**, 1165 (1998).
18. Belyaev V.S. et al. *Zh. Eksp. Teor. Fiz.*, **98**, 1133 (2004).